Insight into $Mg(BH_4)_2$ with Synchrotron X-ray Diffraction: Structure Revision, Crystal Chemistry, and Anomalous Thermal Expansion

Yaroslav Filinchuk,*,† Radovan Černý,*,‡ and Hans Hagemann§

Swiss-Norwegian Beam Lines at ESRF, BP-220, 38043 Grenoble, France, and Laboratory of Crystallography and Department of Physical Chemistry, University of Geneva, 1211 Geneva, Switzerland

Received November 6, 2008. Revised Manuscript Received January 14, 2009

Pure $Mg(BH_4)_2$ has been characterized by single-crystal and powder synchrotron X-ray diffraction and by vibrational spectroscopies. The earlier reported $P6_1$ structure of the α-phase is revised in the space group $P6_122$. Location of the H-atoms from powder data in the published $P6_1$ models posed the main problem for the identification of the correct symmetry: wrongly determined orientations of some BH_4 groups hampered a successful detection of the true $P6_122$ symmetry. Four nearly ideally tetrahedral BH_4 groups form a dodecahedral MgH_8 coordination around each Mg atom, which can be described as a slightly distorted snub disphenoid, where two nearly planar BH_2-Mg-H_2B fragments are situated at ∼90° dihedral angle. The H···H distances between two BH_4 groups within the BH_2-Mg-H_2B fragments are among the shortest (2.18−2.28 Å) in the structurally characterized metal borohydrides. α-$Mg(BH_4)_2$ contains an unoccupied void, accounting for 6.4% of space in the structure. It is large enough (37 $Å^3$) to accommodate a small molecule, such as H_2O. The high-temperature β-phase is less dense by ∼3% but contains no unoccupied voids. The α-phase transforms into the β-phase above 490 K; the latter is quenched (metastable) on cooling. The anomalous cell expansion of the β-phase down to 100 K may be related to the evolution of the free energy profile far from the phase transition temperature.

Introduction

Because of high gravimetric hydrogen density, metal borohydrides are seen as promising materials for energy storage. Indeed, some borohydrides desorb a large quantity of hydrogen (up to 20.8%), although the decompositon temperatures are usually high.[1] Magnesium borohydride currently attracts a particular interest. The Pauling electronegativity of magnesium is higher than of the alkaline metals, and given its empirical relation with the enthalpy of formation,[2] this makes $Mg(BH_4)_2$ more interesting for hydrogen storage applications than MBH_4 (M = Li, Na, K).

Two experimental studies of $Mg(BH_4)_2$ structures were done recently: one by a combination of the synchrotron and neutron powder diffraction techniques on the hexagonal α-phase[3] and the other by the synchrotron X-ray powder diffraction on the α-phase and on the high-temperature orthorhombic β-phase.[4] Subsequent theoretical works were focused on the experimentally observed phases [5,6] and were aiming to predict other stable modifications of magnesium borohydride.[7] The $P6_1$ symmetry of the α-phase [3,4] was questioned in ref 5 but was not in refs 6 and 7.

Thermal decomposition of $Mg(BH_4)_2$ proceeds via several steps, as revealed by TG-DTA-DSC[8] and by TG-PCT.[9] The only in situ diffraction work[10] also aimed to study the decomposition routes, leaving the temperature evolution of the $Mg(BH_4)_2$ phases (e.g., thermal expansion) out of the scope of the investigation. However, the theoretical estimates of the enthalpy of the decomposition [6,7] indicate that the thermodynamics of the hydrogen desorption from $Mg(BH_4)_2$ is close to that of an ideal hydrogen storage material, suggesting the latter may be well suited for reversible hydrogen storage.

To resolve the symmetry ambiguity for the α-phase, we decided to employ single-crystal diffraction. This is the technique which we recently successfully applied to other metal borohydride systems.[11−13] Following our observation

* Corresponding authors. E-mail: yaroslav.filinchuk@esrf.fr; radovan.cerny@unige.ch. Tel.: +33 47 688 2775. Fax: +33 47 688 2694. Tel.: +41 22 379 6450. Fax: +41 22 379 6108.
† Swiss-Norwegian Beam Lines at ESRF.
‡ Laboratory of Crystallography, University of Geneva.
§ Department of Physical Chemistry, University of Geneva.

(1) Soloveichik, G. *Mater. Matters (Aldrich)* **2007**, *2*, 11–14.
(2) Nakamori, Y.; Miwa, K.; Ninomiya, A.; Li, H.; Ohba, N.; Towata, S.; Züttel, A.; Orimo, S. *Phys. Rev. B* **2006**, *74*, 045126.
(3) Černý, R.; Filinchuk, Y.; Hagemann, H.; Yvon, K. *Angew. Chem., Int. Ed.* **2007**, *46*, 5765–5767.
(4) Her, J.-H.; Stephens, P. W.; Gao, Y.; Soloveichik, G. L.; Rijssenbeek, J.; Andrus, M.; Zhao, J.-C. *Acta Crystallogr., Sect. B* **2007**, *63*, 561–568.
(5) Dai, B.; Sholl, D. S.; Johnson, J. K. *J. Phys. Chem. C* **2008**, *112*, 4391–4395.
(6) van Setten, M. J.; de Wijs, G. A.; Fichtner, M.; Brocks, G. *Chem. Mater.* **2008**, *20*, 4952–4956.
(7) Ozolins, V.; Majzoub, E. H.; Wolverton, C. *Phys. Rev. Lett.* **2008**, *100*, 135501.
(8) Hanada, N.; Chłopek, K.; Frommen, Ch.; Lohstroh, W.; Fichtner, M *J. Mater. Chem.* **2008**, *18*, 2611–2614.
(9) Li, H.-W.; Kikuchi, K.; Nakamori, Y.; Ohba, N.; Miwa, K.; Towata, S.; Orimo, S. *Acta Mater.* **2008**, *56*, 1342–1347.
(10) Riktor, M. D.; Sørby, M. H.; Chłopek, K.; Fichtner, M.; Buchter, F.; Züttel, A.; Hauback, B. C. *J. Mater. Chem.* **2007**, *17*, 4939–4942.
(11) Filinchuk, Y. E.; Yvon, K.; Meisner, G. P.; Pinkerton, F. E.; Balogh, M. P. *Inorg. Chem.* **2006**, *45*, 1433–1435.
(12) Filinchuk, Y.; Hagemann, H. *Eur. J. Inorg. Chem.* **2008**, 3127–3133.
(13) Filinchuk, Y.; Chernyshov, D.; Černý, R. *J. Phys. Chem. C* **2008**, *112*, 10579–10584.

10.1021/cm803019e CCC: $40.75
Published on Web 02/06/2009

of grain growth below the α → β phase transition, we annealed the sample of α-$Mg(BH_4)_2$ and succeeded in obtaining single crystals sufficiently large for the diffraction study, while the use the synchrotron radiation yielded high-quality data. The latter provided a wealth of new reliable information, in particular with respect to position of hydrogen atoms, enabling us to correct the symmetry and some structural details of the α-phase and make a few important observations on the crystal chemistry of magnesium borohydride. We also compared the results of different diffraction techniques and of the DFT calculations. α- and β-$Mg(BH_4)_2$ phases were studied by in situ powder diffraction within 100−500 K range, uncovering an anomalous thermal expansion behavior. Also, for the first time, the neat 100% pure sample was characterized by Raman and infrared spectroscopies, showing a difference with the measurements done on KBr + $Mg(BH_4)_2$ pellets.

Experimental Section

Synthesis of Pure $Mg(BH_4)_2$. The title compound was prepared according to a modified synthesis procedure outlined in ref 14. About 12 mL of triethylamine−borane was added under dry nitrogen atmosphere to 1 g of milled MgH_2 (milling time 2 h). The mixture was heated for 1 h to 100 °C and then for 6 h to 145 °C, observing a substantial evolution of gas. After cooling, a black mass was obtained. Thirty milliliters of hexane were added, and the mixture was left to stand overnight. As the mass remained compact, the hexane was evaporated under vacuum and $Mg(BH_4)_2$ was extracted from the mass by adding about 100 mL of diethyl ether. The resulting suspension was decanted, and the supernatant ether solution was evaporated to yield a small amount of solid which was dried over several days under vacuum at increasing temperatures of up to 130 °C, similar to our previously reported synthesis.[3] X-ray diffraction confirmed 100% purity of the sample.

Single-Crystal Diffraction. A crystal of ∼50 μm size has been selected from the powder sample which was annealed for one week under 1 bar of argon at 453 K. The crystal was selected under a protective layer of oil and rapidly transferred to a 100 K nitrogen stream. Diffraction measurements were done at the Swiss-Norwegian Beam Lines (SNBL) at the European Synchrotron Radiation Facility (ESRF). Diffraction data were taken at 100 K using the MAR345 Image Plate detector, at the wavelength 0.770294 Å and the crystal-to-detector distance of 150 mm. A total of 219 frames with 1° rotation and 10 s exposure time have been collected. All diffraction intensities could be indexed in a primitive hexagonal lattice. A total of 18 572 diffraction intensities were integrated using CrysAlis software.[15] A highly redundant data set (∼99.8% completeness, more than 13 equiv or repetitive measurements per unique reflection up to 0.95 Å resolution) was obtained. The data were corrected for Lorentz factor and polarization effects. Absorption correction and scaling of frames for the decaying intensity of the synchrotron beam were performed using SADABS.[16] The structure was refined with SHELXL[17] using the suggested $P6_122$ structure[5] as a starting model. Mg and B atoms were refined anisotropically, while the H atoms were refined isotropically without any constraints. Neutral atom scattering factors were used. PLATON[18] did not detect higher metric or crystallographic symmetry than $P6_122$ but revealed a void at $x = 0.093$, $y = 0.186$, and $z = 0.250$ with the shortest distance to the nearest atoms (H) of about 2.7 Å. Refinement shows that the void is unoccupied.

Crystal data: $Mg(BH_4)_2$, $M = 53.994$ g/mol, hexagonal, space group $P6_122$, $a = 10.3540(12)$, $c = 37.055(4)$ Å, $V = 3440.3(7)$ Å^3, $Z = 30$, $\rho_c = 0.782$ g/cm^3, $\mu = 0.16$ mm^{-1}, $T = 100$ K, $R_{int} = 0.0635$, $R_\sigma = 0.0240$. 150 refined parameters, $R_1 = 0.0408$ and w$R_2 = 0.0929$ for 1323 independent reflections with $I > 2\sigma(I)$; $R_1 = 0.0445$ and w$R_2 = 0.0952$ for all 1411 independent reflections (Friedel pairs not merged), GoF = 1.180, Flack parameter 0.0(6), $\Delta\rho_{max/min} = 0.14(4)/-0.17(4)$ e/Å^3.

In Situ Powder Diffraction. Diffraction data for the polycrystalline sample were collected on a 0.5 mm glass capillary filled in a high purity Ar atmosphere with a fine powder of $Mg(BH_4)_2$. A MAR345 Imaging Plate detector at the sample-to-detector distance of 250 mm and synchrotron radiation at $\lambda = 0.770294$ Å were used. The capillary was heated from 100 to 500 K and then cooled down to 100 K at a 120 K per hour rate, while synchrotron powder diffraction data were collected in situ. Temperature was controlled with an Oxford Cryostream 700+. Each pattern was collected during 60 s exposure time, while the capillary was rotated by 60°, followed by a readout during 83 s. The data were integrated using Fit2D program[19] and a calibration measurement of a NIST LaB_6 standard sample. Rotation of the sample during the measurement and integration of the diffraction rings provides very good powder averaging. Uncertainties of the integrated intensities were calculated at each 2θ-point by applying Poisson statistics to the intensity data, considering the geometry of the detector, similar to the procedure described in ref 20.

Rietveld refinement for the α-phase was based on the atomic coordinates we determined from the single-crystal diffraction data and for the β-phase on the structural data reported in ref 4 for the *Immm* average of the *Fddd* structure. All atomic parameters were fixed, while the cell and profile parameters were refined sequentially using Fullprof.[21] This yielded the temperature dependence of the unit cell parameters for the low- and high-temperature phases of $Mg(BH_4)_2$. The cell parameters refined for the *Immm* model ($^1/_2 \times {}^1/_2 \times {}^1/_2$ of the true unit cell) were finally doubled. The typical fit of the $P6_122$ structure to the image-plate powder diffraction data is illustrated in Figure S1 (Supporting Information) with a pattern collected at 92 K.

High-Resolution Powder Diffraction. High-resolution powder diffraction data were collected at room temperature on the 0.5 mm glass capillary filled with the same powder. The synchrotron radiation (Materials Science Beamline at the SLS, PSI) at $\lambda = 0.880114$ Å and silicon strip detector MYTHEN II were used. Twenty-two powder patterns at two different detector positions were collected for 5 s each and then binned into one pattern. The diffractometer was calibrated with an external silicon standard.

The structure was refined using the TOPAS Academic[22] and the single-crystal results as a starting model. The displacement parameters of magnesium and boron atoms were refined anisotropically; one common isotropic displacement factor was refined for hydrogen atoms. The BH_4 groups occupying general positions were

(14) Chłopek, K.; Frommen, Ch.; Léon, A.; Zabara, O.; Fichtner, M *J. Mater. Chem.* **2007**, *17*, 3496–3503.
(15) Oxford Diffraction. *CrysAlis Software Package*; Oxfordshire, U.K., 2006.
(16) Sheldrick, G. M. *SADABS*; University of Göttingen: Göttingen, Germany, 1997.
(17) Sheldrick, G. M. *SHELXS97 and SHELXL97*; University of Göttingen: Göttingen, Germany, 1997.
(18) Spek, A. L. *PLATON*; University of Utrecht: Utrecht, The Netherlands, 2006.
(19) Hammersley, A. P.; Svensson, S. O.; Hanfland, M.; Fitch, A. N.; Häusermann, D. *High Pressure Res.* **1996**, *14*, 235–248.
(20) Vogel, S.; Ehm, L.; Knorr, K.; Braun, G. *Adv. X-ray Anal.* **2002**, *45*, 31–33.
(21) Rodriguez-Carvajal, J. *FULLPROF SUITE*; LLB Sacley & LCSIM: Rennes, France, 2003.
(22) Coelho, A. A. *J. Appl. Crystallogr.* **2000**, *33*, 899–908.

Table 1. Essential Interatomic Distances (Å) and Angles (deg) in α-Mg(BH4)2, As Found in the Space Group *P*6$_1$ in Earlier Powder Diffraction Studies,[3,4] DFT,[5] and Our Diffraction Studies in *P*6$_1$22

		method				
		synchrotron + neutron powder diffraction	synchrotron powder diffraction	DFT	single-crystal synchrotron diffraction	synchrotron powder diffraction
temperature		293 K; 173 K	ambient	0 K	100 K	ambient
space group		*P*6$_1$	*P*6$_1$	*P*6$_1$22	*P*6$_1$22	*P*6$_1$22
reference		3	4	5	this work	this work
Mg−B	max	2.53	2.57	2.416	2.437(4)	2.448
	min	2.31	2.28	2.382	2.400(5)	2.391
	av	2.42	2.42	2.404	2.424	2.418
Mg−H	max	2.45	2.66	2.13	2.16(4)/2.16[a]	2.19
	min	1.80	1.76	2.00	1.93(4)/1.92[a]	1.91
	av	2.03	2.04	2.05	2.03/2.02[a]	2.02
B−H	max	1.18	1.13	1.23	1.22(3)/1.30[a]	1.12
	min	1.18	1.12	1.22	1.08(3)/1.16[a]	1.12
	av	1.18	1.12	1.224	1.142/1.224[a]	1.117(7)
H−B−H	max	109.5	110.0	115.9	115.4(27)	115.2
	min	109.5	109.0	105.7	102.2(24)	100.0
	av	109.5	109.5	109.5	109.5	109.4
B−Mg−B	max	131.10	137.39	129.40	129.01(13)	129.31
	min	82.83	91.75	91.81	92.10(14)	92.42
	av	109.69	109.73	109.94	109.98	109.97
Mg−B−Mg	max	177.44	175.45	170.92	169.84(17)	169.53
	min	147.94	143.88	148.94	148.13(19)	147.81
	av	158.16	160.14	161.55	161.03	161.36
B−H−Mg	max	111.8	119.6	92.5	102(2)/99.6[a]	102.6
	min	79.8	73.3	86.1	88(2)/86.4[a]	87.2
	av	94.8	96.3	90.8	95.8/93.5[a]	96.8

[a] Using positions of H-atoms corrected for ~0.08 Å X-ray shortening[13] of the B−H distances.

refined as rigid ideally tetrahedral units, using the same B−H distance for all the BH_4 groups as the only varied parameter. The uncertainties of crystallographic coordinates of hydrogen atoms were therefore not available from the least-squares matrix and were estimated by the bootstrap method.[23] For the *P*6$_1$22 model, the agreement factors are R_{wp} (not corrected for background) = 0.65%, R_p (corrected for background) = 7.12%, χ^2 = 4.69, and R_{Bragg} = 0.17%. The B−H distance was refined to 1.117(7) Å. The fit of the *P*6$_1$22 structure to the high-resolution powder diffraction data is shown in Figure S2 (Supporting Information). A similar refinement has been attempted for comparison in the space group *P*6$_1$, which involves almost twice as many variables as in *P*6$_1$22, and yields similar agreement factors: R_{wp} (not corrected for background) = 0.64%, R_p (corrected for background) = 7.22%, χ^2 = 4.64, and R_{Bragg} = 0.24%.

IR and Raman Spectroscopy. Infrared measurements on the neat powder samples were done using a Specac "Golden Gate" ATR cell in a Perkin-Elmer Spectrum One instrument with a nominal resolution of 2 cm^{-1}. The samples were loaded into the ATR cell in an argon-filled glovebox. Raman spectra were obtained using a Labram Raman microscope (with 532 nm excitation) on the samples sealed in glass capillaries; the spectral resolution was 3−4 cm^{-1}.

Results and Discussion

Our single-crystal diffraction study shows that the true symmetry of α-Mg(BH4)2 is higher than it was originally reported by two independent groups from powder diffraction data.[3,4] The space group is revised from polar *P*6$_1$ to nonpolar *P*6$_1$22, in agreement with a suggestion made by Dai et al.,[5] based on the DFT optimization of the experimental *P*6$_1$ structure. High accuracy and precision of the structural parameters obtained by single-crystal diffraction allows us first to compare the results of different diffraction techniques and of the DFT calculations and then to focus on the crystal chemistry of magnesium borohydride, trying to understand which building principles are the driving forces defining such a complex structure of the seemingly simple system. This will help to understand better the stability of the light metal borohydrides.

Comparison of Structural Data Obtained by Various Techniques. The main distances and angles in α-Mg(BH4)2 determined by various diffraction techniques in the space groups *P*6$_1$ and *P*6$_1$22 and by DFT optimization of the experimental structure are presented in Table 1. Atomic coordinates found in the DFT study and in this work are standardized and put for comparison in Table S1 of the Supporting Information. The differences in atomic positions between the DFT-optimized and our experimental *P*6$_1$22 structures (both from the single crystal and powder diffraction) are listed in Table S2 (Supporting Information).

The comparison shows that the DFT-optimized and single-crystal structures are very close: positions of the individual atoms differ by 0.06 to 0.37 Å, with a mean difference of 0.16 Å. Assuming the corrected positions of H-atoms (see below in the text) the differences decrease to 0.05−0.32 Å with the mean of 0.14 Å. The largest differences are observed for the two BH_4 groups occupying the special positions on the 2-axis (atoms B1 and B2): the mean difference for these groups is 0.24 Å, compared to 0.12 Å for the remaining atoms.

Our new synchrotron powder diffraction data, collected on the single-phase sample, result in a very good agreement with the single-crystal structure (see Table 1S, Supporting Information). Differences between the Rietveld refined atomic coordinates and those obtained in the single-crystal

(23) Efron, B.; Tibshirani, R. *Stat. Sci.* **1986**, *1*, 54–77.

and DFT studies (see Tables S1 and S2 in the Supporting Information for comparison) show a 0.01−0.34 Å spread, with a mean of 0.17 Å. Thus, the restrained refinement using high-resolution powder data collected on the 100% pure sample allows us to approach the accuracy of the single-crystal study. We should note, however, that Rietveld refinement with random initial BH_4 orientations converged to a different local minimum, where at least one BH_4 group is flipped comparing to the single-crystal structure. The best *R*-factors (the global minimum) were achieved only when the restrained Rietveld refinement was started with the initial coordinates of the single-crystal structure. Thus, even high-quality synchrotron powder data, when used alone, do not allow to determine reliably orientation of all the BH_4 groups in α-$Mg(BH_4)_2$.

We used the Addsym procedure in Platon[18] to quantify the deviation of the $Mg(BH_4)_2$ structure refined in the space group $P6_1$ from the $P6_122$ average. With the single-crystal data, the maximal deviation of atomic positions in $P6_1$ model from the $P6_122$ average is 0.09 Å. Powder diffraction provides lower accuracy: using our new SLS data collected on the single-phase sample, we find 0.35 Å maximal deviation of the refined $P6_1$ model from the $P6_122$ average. The previously published powder diffraction studies suffer from similar problems: 94% of the $P6_1$ structure model refined from the combination of synchrotron and neutron powder data[3] show less than 0.53 Å deviations of atomic positions from the $P6_122$ average. However, deuterium atoms of one of the BD_4 groups (occupying the special position in $P6_122$) show a strong disagreement with the $P6_122$ structure. A comparable discrepancy is observed for the $P6_1$ structure model refined from the synchrotron powder data only,[4] where most of the atoms reveal less than 0.49 Å deviations from the $P6_122$ average, while hydrogen atoms of three BH_4 groups do not fit the $P6_122$ symmetry.

In all four cases, the largest differences involve hydrogen atoms. Magnesium and boron atoms can be located with high accuracy even in the $P6_1$ model using powder diffraction data: these atoms show only a marginal difference with the $P6_122$ average and with the theoretically optimized structure.[5] In contrast to the heavier atoms, hydrogen posed the main problem for the identification of the correct symmetry: some incorrect orientations of the BH_4 groups in the space group $P6_1$ were trapped in a local and probably rather flat minimum of the corresponding cost functions, first during the global optimization of the structure solution and later during the Rietveld refinement. Thus the $P6_1$ model was technically far from the $P6_122$ average, and this hampered a successful detection of the true $P6_122$ symmetry by automatic algorithms, such as Addsym in Platon.[18]

We should note also that the refinement in $P6_1$ involves almost twice as many variables as in $P6_122$. Any difference between the calculated and observed intensities, including all kinds of random and systematic errors, is reduced by refining more variables in $P6_1$ than in $P6_122$. In powder diffraction patterns, the full overlap of the *hkl* and *khl* reflections, equivalent in $P6_122$ but inequivalent in $P6_1$, impedes resolving this ambiguity. Single-crystal diffraction, where these reflections are measured separately, is more stable with respect to this bias: R_1 factor for the $P6_1$ model is even higher than for the true $P6_122$ symmetry—4.18% for 297 parameters versus 4.07% for 151 parameters. Thus, the large uncertainties in H-atoms' positions determined in $P6_1$ were the main reason for missing the true $P6_122$ symmetry.

B−H Distances. Twenty independent B−H distances, experimentally determined on the single crystal, cover the range from 1.08(3) to 1.22(3) Å, with the 1.142 Å mean. Its standard deviation, 0.038 Å, estimated from the scatter of the observations, is the same as the uncertainties for the individual B−H distances obtained from the least-squares refinement (0.03−0.04 Å). Also, there is no correlation between B−H and H···Mg distances or B−H···Mg angles. The absence of statistically detectable differences implies that all the BH_4 groups manifest identical B−H bond lengths. This agrees with the conclusions made from other accurate experimental studies of light borohydrides[11−13] and with the theoretical study of $Mg(BH_4)_2$[5] finding all the B−H distances equal within 0.01 Å.

The average B−H distance determined from the single-crystal X-ray diffraction at 100 K is quite accurate: the standard error of the mean (1.142 Å) is 0.008 Å. The experimental average is 0.082 Å shorter than the theoretical one (1.224 Å [5]). Detailed study of the simple metal borohydrides structures [12,13] showed that ∼0.08 Å of this difference originates from the displacement of the electron cloud seen by X-rays relative to an average nuclear position. The refined atomic displacements of B and H-atoms in $Mg(BH_4)_2$ at 100 K are very similar, suggesting that the libration of the BH_4 units is small and therefore an apparent shortening of the B−H bonds due to this geometric effect is indeed insignificant. This view finds a support from the powder diffraction study at room temperature: the common B−H distance refined for all the BH_4 groups is only slightly shorter, 1.117(7) Å, than the 1.142(8) Å mean at 100 K. Thus, the apparent shortening of the B−H distances due to an increased BH_4 libration when going from 100 K to the room temperature is rather small (∼0.025 Å). To evaluate better the geometry of the BH_4···Mg interaction (see below) and to compare directly our experimental results with the DFT calculations (see Table S2, Supporting Information), the apparent hydrogen atom positions at 100 K were corrected by extending the average experimental B−H bond lengths by 0.082 Å. The list of corrected positions is given in Table S1 (Supporting Information). Below we will discuss geometrical characteristics using the corrected coordinates of the H atoms.

Coordination of the BH_4 Groups. The tetrahedral BH_4 groups are coordinated by Mg atoms via the two opposite edges. The resulting Mg−H_2B bridges are approximately flat, and this results in relatively long Mg−B distances, which cover a very narrow range from 2.400(4) to 2.437(4) Å, as well as maximizes the Mg···Mg distances so that the shortest one exceeds 4.65 Å. However, the deviation of a Mg atom from the plane defined by the three atoms belonging to the coordinated H_2B edge can be as large as 1 Å, as for instance for Mg atoms near B1 and B6. Thus, the resulting Mg−H_2BH_2−Mg fragments are not strictly linear: the

Mg−B−Mg angles range 148−170° (see Table 1 for more details).

H−B−H Angles. Single-crystal data show that the H−B−H angles in the Mg−H$_2$B fragments are slightly more open than for the noncoordinated H$_2$B edge, where two H-atoms do not bond to the same Mg: the respective angles are 110.8° (average over 12 values) versus 108.8° (average over 24 values). The spread of H−B−H angles for the Mg-coordinated edges is three times smaller than for the noncoordinated ones, suggesting that the latter are more prone to distortion, while the coordinated H$_2$B fragments are more rigid.

In the DFT-optimized α-Mg(BH$_4$)$_2$, the Mg-coordinated H$_2$B fragments reveal much more open H−B−H angles (115.3°,[5] 115(1)° [6]) than the noncoordinated ones (106.7°,[5] 107(1)° [6]). Again, the spread of the H−B−H angles for the coordinated edges of BH$_4$ is almost two times smaller than for the noncoordinated ones. Thus, the DFT model shows the same trend, revealing even the larger difference: the mean experimental difference between the Mg-coordinated and noncoordinated H−B−H angles is 2.0°, while the calculated model gives more than 8°. The differences are statistically significant: the standard error of the mean is 0.50−0.75° for the experiment and 0.11−0.12° for the theoretically optimized structure. The smaller difference observed in the experiment is likely caused by the displacement of the electron cloud seen by X-rays relative to the nuclear position of the hydrogen atoms. The DFT study of the similar compound, Be(BH$_4$)$_2$,[24] reveals that the charge density in the Be−H$_2$B fragments is clearly shifted toward the center of the Be−H$_2$−B rhomb: it results in smaller H−B−H angles for the coordinated H$_2$B group, when estimated from the centers of the electron clouds comparing to the actual nuclear positions. A similar experimentally detected distortion of the BH$_4$ groups, which correlates with the results of the electron diffraction studies in the gas phase and of the DFT calculations, was observed for Al(BH$_4$)$_3$ structures.[25] This distortion can be attributed to the strong polarizing effect of the M^{2+} and M^{3+} cations or to a partially covalent M−BH$_4$ interaction.

Coordination of Mg Atoms. Mg atoms clearly take an intermediate position between the smaller beryllium atoms, which are surrounded by three BH$_4$ groups in Be(BH$_4$)$_2$,[26] and the larger calcium atoms taking an octahedral coordination in three structurally characterized Ca(BH$_4$)$_2$ phases.[27−29] The strongly deformed tetrahedral environment of Mg atoms by four BH$_4$ groups was found in the original $P6_1$ structure models.[3,4] In the revised $P6_122$ structure, the B−Mg−B angles fall in a narrower range (92−129°, see Table 1 for comparison), but the [Mg(BH$_4$)$_4$] tetrahedra remain severely distorted. The high accuracy of the single-crystal structure allows us to analyze the coordination geometry of Mg with respect to the hydrogen atoms. The geometry of [Mg(BH$_4$)$_4$] is very similar for each of the three independent Mg atoms, so it is shown in Figure 1 only for Mg2. The four BH$_4$ groups around Mg can be grouped in two pairs, each forming a BH$_2$−Mg−H$_2$B fragment, and the two fragments form the right dihedral angle. The least-squares (LS) planes characterizing geometry of the three coordination spheres are listed in the Supporting Information. The BH$_2$−Mg−H$_2$B fragments are approximately planar: the largest atomic deviation from the LS planes is 0.2 Å, and the dihedral angles between the fragments are within the 85(1)−87.8(7) range.

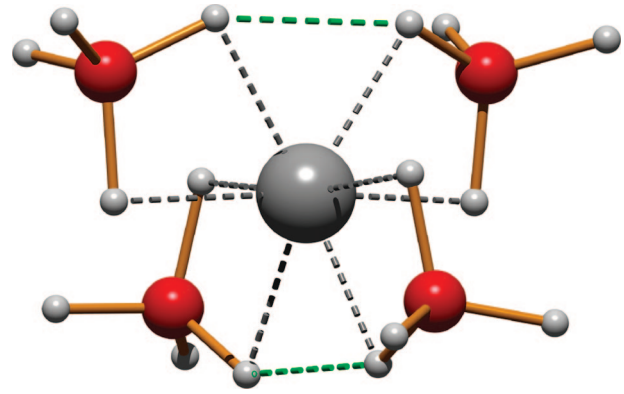

Figure 1. Geometry of [Mg(BH$_4$)$_4$] units in α-Mg(BH$_4$)$_2$, coordination of Mg2 atom is given as an example. Two nearly planar BH$_2$−Mg−H$_2$B fragments are situated at nearly 90° dihedral angle. The shortest H···H distances are highlighted in green.

The MgH$_8$ coordination polyhedra in α-Mg(BH$_4$)$_2$ have 12 faces, so they can be generally called dodecahedra, but more precisely they are slightly distorted snub disphenoids (see Figure S3, Supporting Information). The long-range packing, based on the MgH$_8$ snub disphenoids and nearly linearly coordinated H$_2$BH$_2$ units, results in screwed (−Mg−BH$_4$−)$_n$ chains of large periodicity which are finally organized into the 3D network involving a large number of 5-membered (−Mg−BH$_4$−)$_5$ rings. Indeed, it was pointed out by Setten et al. [6] that a much simpler Cu$_2$O-type structure of Mg(BH$_4$)$_2$, proposed in ref 3, is impossible with these local geometries. However, it has passed unnoticed that MgH$_8$ polyhedra in the *Fddd* polymorph of Mg(BH$_4$)$_2$ (β-phase) have a different geometry, that is, slightly distorted biaugmented triangular prism (see Figure S3, Supporting Information) for one independent Mg atom and gyrobifastigium (see Figure S3, Supporting Information) for the other. These two polyhedra have 9 and 8 faces, respectively, and they allow for completely different topology of (−Mg−BH$_4$−)$_n$ chains and rings; in particular, no odd-membered rings are observed in β-Mg(BH$_4$)$_2$. While the formation of the complex $P6_122$ structure is closely related to the dodecahedral MgH$_8$ configuration, we still see the hypothetical Cu$_2$O-type structure possible with different MgH$_8$ geometries.

The BH$_4$ groups are held by strong covalent bonds, so the intramolecular H···H distances (within the BH$_4$ groups)

(24) van Setten, M. J.; de Wijs, G. A.; Brocks, G. *Phys. Rev. B* **2008**, *77*, 165115.
(25) Aldridge, S.; Blake, A. J.; Downs, A. J.; Gould, R. O.; Parsons, S.; Pulham, C. R. *J. Chem. Soc., Dalton Trans.* **1997**, 1007–1012.
(26) Marynick, D. S.; Lipscomb, W. N. *Inorg. Chem.* **1972**, *11*, 820–823.
(27) Miwa, K.; Aoki, M.; Noritake, T.; Ohba, N.; Nakamori, Y.; Towata, S.-i.; Züttel, A.; Orimo, S.-i. *Phys. Rev. B* **2006**, *74*, 155122.
(28) Buchter, F.; Łodziana, Z.; Remhof, A.; Friedrichs, O.; Borgschulte, A.; Mauron, Ph.; Züttel, A.; Sheptyakov, D.; Barkhordarian, G.; Bormann, R.; Chłopek, K.; Fichtner, M.; Sørby, M.; Riktor, M.; Hauback, B.; Orimo, S. *J. Phys. Chem. B* **2008**, *112*, 8042–8048.
(29) Filinchuk, Y.; Rönnebro, E.; Chandra, D. *Acta Mater.* **2009**, *57*, 732–738.

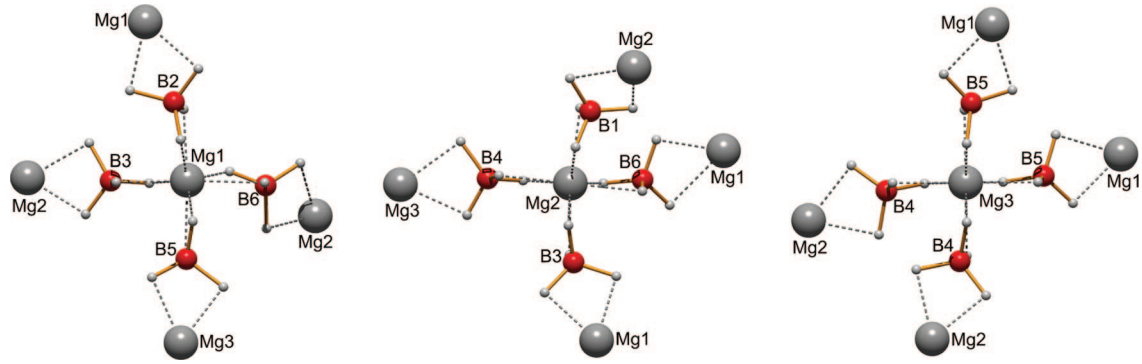

Figure 2. Deviation from the ideal coordination geometries for Mg atoms and for the BH_4 groups.

lie in the narrow 1.88−2.13 Å range, with the 2.00 Å average. The intermolecular H···H contacts, on the other hand, are largely defined by the MgH_8 coordination geometry. Analysis based on the corrected positions of H-atoms reveals that the shortest H···H distances between the BH_4 groups appear within the planar BH_2-Mg-H_2B fragments, highlighted in green in Figure 1. The length of the five independent H···H contacts of this type ranges from 2.18 to 2.28 Å, with the mean of 2.24 Å. These intermolecular H···H contacts are among the shortest in the structurally characterized borohydrides of light metals;[30] a shorter distance was observed only in the high-pressure polymorph of $LiBH_4$.[31] All other intermolecular H···H contacts in α-$Mg(BH_4)_2$ are longer than 2.47 Å but typically range from 2.7 to 2.9 Å.

Mg−H distances in α-$Mg(BH_4)_2$, as described originally in the space group $P6_1$,[3,4] showed very large spread (see Table 1), if we assume BH_4 coordination by Mg via the edges. Table 2 in ref 5 lists only the lower range of Mg−H distances, thus yielding a strongly underestimated 1.85 Å average, leading to a fictitious contradiction with theory. Actually, the average Mg−H distances determined by different techniques are similar, and only the spread of values differs (see Table 1). The single-crystal study gives a 1.92−2.16 Å range, which is only slightly broader than the 2.00−2.13 Å range found theoretically. Experimentally determined Mg−H distances linearly correlate with B−H−Mg angles, in a very similar way as in the DFT-optimized structure (see Figure S4, Supporting Information). Variation of Mg···H distances and the deformation of the BH_2-Mg-H_2B planes from the ideal values allows certain flexibility in a mutual orientation of the $[Mg(BH_4)_4]$ tetrahedra. Combined with the deformation of the pseudolinear $Mg-H_2BH_2-Mg$ fragments, this leads to a significant deviation from the ideal coordination geometries for Mg atoms and for the BH_4 groups, as illustrated in Figure 2. Small but ubiquitous deviations from the ideal coordination geometries presumably allow the structure to pack more densely. However, we have unexpectedly discovered empty voids in this seemingly ionic structure.

Unoccupied Voids. Using a probe of 1.2 Å radius in Platon[18] and assuming a 1.2 Å van der Waals radius of the hydrogen atom, a void was detected in the $P6_122$ structure determined from the single crystal diffraction data. The void is located in a Wyckoff site 6*b* (x $2x$ $^1/_4$) at $x = 0.093$. This point is 2.76 Å apart from the nearest (H) atom (2.71 Å using the corrected positions of H-atoms). A detailed examination revealed that the void may host even a bigger atom: a point at $x = 0.105$ has its 12 shortest contacts to H-atoms at 2.91−3.29 Å (2.86−3.25 Å using the corrected positions of H-atoms), 8 contacts to B-atoms at 3.40−4.08 Å, and the shortest contact to Mg is 3.70 Å. An analysis with a probe of 1.0 Å radius shows that this void accounts for 7.5% of space in the structure; this estimate is lowered to 6.4% considering the corrected positions of H-atoms.

A possible collapse of the unoccupied void might contribute significantly to a volume drop upon a hypothetical transition to a denser phase at high pressures. The large void volume of 43 Å^3 (37 Å^3 taking the corrected positions of H-atoms) allows us to consider it to be solvent accessible: it is sufficiently large to accommodate a small molecule, such as H_2O.

Importantly, the void forms a spiral around the 6_1 axis, with 6.47 Å distance between the symmetry-related voids. This creates an infinite channel along 00z direction, which may provide a path for hydrogen diffusion during initial stages of hydrogen desorption. It is remarkable that the high-temperature β-phase, crystallizing in the space group *Fddd*,[4] contains no unoccupied voids.

Anisotropy of Thermal Expansion of α- and β-$Mg(BH_4)_2$. Cell parameters, refined from the in situ diffraction data, are shown in Figure 3. First, we wish to clarify that there is a no disagreement between the cell parameters determined in the two previous experiments [3,4] and in this work. The cell parameters given in ref 4 for the two phases at ambient conditions ($a = 10.3414(4)$, $c = 37.086(2)$ Å, $V = 3434.7(3)$ Å^3 for the hexagonal phase and $a = 37.072(1)$, $b = 18.6476$ (6), $c = 10.9123$ (3) Å, $V = 7543.8(5)$ Å^3 for the orthorhombic phase) perfectly match our data plotted in Figure 3. As pointed out in ref 6, the cell parameters for the hexagonal phase listed in ref 3 (at 293 K: $a = 10.3182(1)$, $c = 36.9983(5)$ Å, $V = 3411.3(1)$ Å^3 for the deuterated sample) are considerably smaller. This difference can be explained by smaller thermal vibrations of the heavier BD_4 anions and, therefore, decreased anharmonicity that determines the thermal expansion at a finite

(30) Filinchuk, Y.; Chernyshov, D.; Dmitriev, V. *Z. Kristallogr.* **2008**, *223*, 649–659.
(31) Filinchuk, Y.; Chernyshov, D.; Nevidomskyy, A.; Dmitriev, V. *Angew. Chem., Int. Ed.* **2008**, *47*, 529–532.

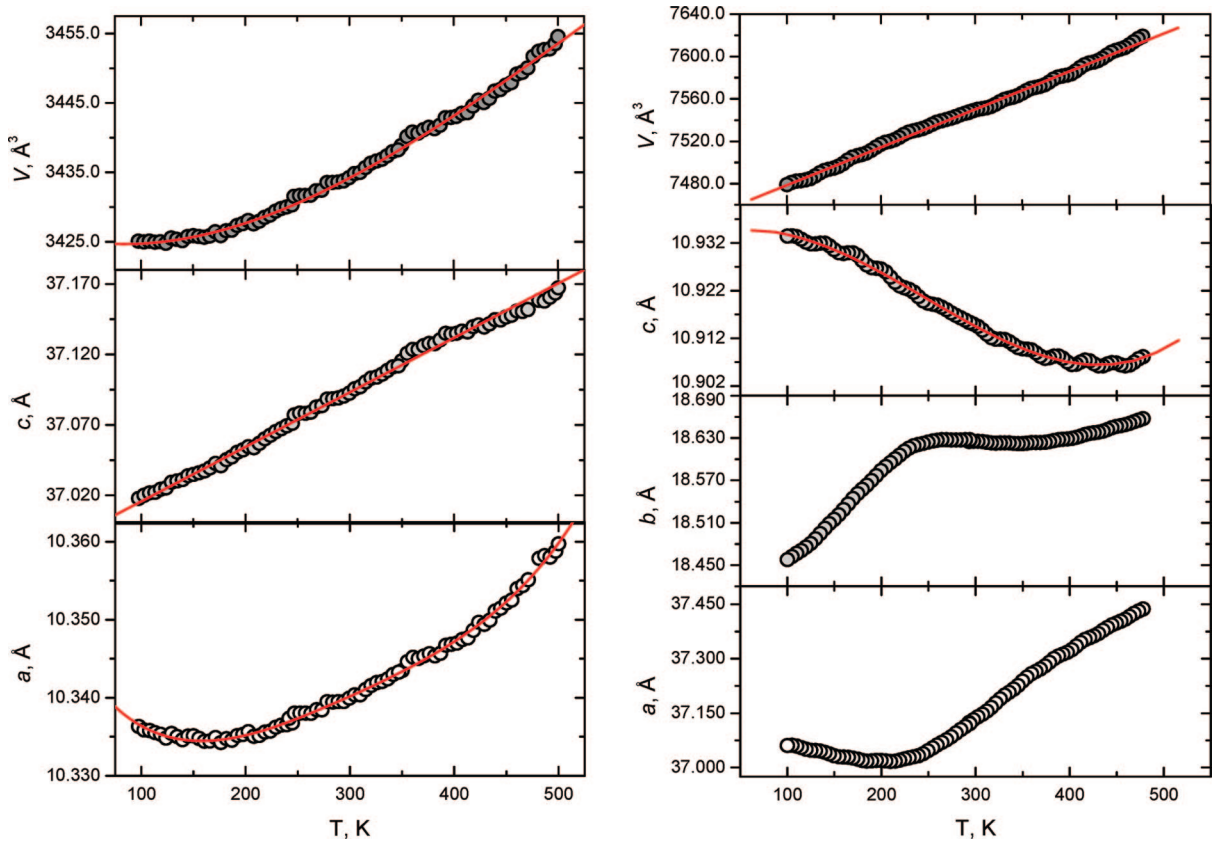

Figure 3. Unit cell volume and cell dimensions of α-$Mg(BH_4)_2$ (left) and β-$Mg(BH_4)_2$ (right), refined from the in situ MAR345 powder diffraction data and plotted as a function of temperature. Polynomial fits (see text) are shown as red lines.

temperature. Similar cell contraction for deuterated derivatives was observed in other metal−borohydride systems.[32]

A smooth variation of the cell parameters for the α-phase indicates that there is no hypothetical transition from the $P6_122$ structure to $P6_1$ or vice versa, supposed in ref 5, and therefore the structure revision for the hexagonal phase is valid at all temperatures.

Our experiments show that the pure α-phase starts to transform into the β-phase at about 490 K and the conversion completes at 500 K within a few minutes. This transition temperature is slightly higher than 453−473 K, reported by Her at el.[4] It is indeed remarkable that the high-temperature β-phase does not transform back to the α-phase when cooled down to 100 K: although the β-phase contains no unoccupied voids, it is by 2.3−3.4% less dense than the α-phase. As illustrated in Figure S5, Supporting Information, the lower limit of this difference corresponds to 100 K and the higher to the transition temperature, slightly below 500 K. At ambient conditions this difference equals 3.0%, in good agreement with the data in ref 4.

Within the 100−500 K temperature range the unit cell parameters for the α-phase can be approximated by the following equations (Å for a and c, $Å^3$ for the cell volume, K for temperature), where the variation of the a parameter is highly nonlinear, with a minimum at ∼170 K:

$$a = 10.356(2) - 3.4(4)\times10^{-4}T + 1.8(2)\times 10^{-6}T^2 - 3.9(6)\times10^{-9}T^3 + 3.2(5)\times10^{-12}T^4$$

$$c = 36.9788(11) + 3.79(3)\times10^{-4}T$$

$$V = 3426.5(11) - 4.4(13)\times10^{-2}T + 2.9(4)\times 10^{-4}T^2 - 1.8(5)\times10^{-7}T^3$$

Thermal expansion for the β-phase is highly anisotropic and very nonuniform: only the cell parameter c and the cell volume V can be approximated by polynomials:

$$c = 10.9320(9) + 8.9(11)\times10^{-5}T - 8.3(4)\times 10^{-7}T^2 - 1.12(5)\times10^{-9}T^3$$

$$V = 7442.7(7) + 0.358(2)T$$

while the fits for a and b are bad for low-order polynomials and give unreasonable values for the high-order ones. Indeed, the cell parameter b reveals very complex temperature behavior: it shows a maximum at about 275 K and a minimum at 345−350 K. The other two cell parameters also show an unusual behavior: a and c display minima at ∼200 and ∼450 K, respectively, increasing toward lower temperatures.

Stability of the two phases in the wide temperature range can be considered as a broad hysteresis, which indicates an existence of two similar energy minima separated by a barrier. The high-temperature β-phase is metastable at low temperatures and can transform into the more stable α-phase (the energy estimates are given in ref 7), but the kinetics of this first-order reconstructive transition slows down with

(32) Renaudin, G.; Gomes, S.; Hagemann, H.; Keller, L.; Yvon, K. *J. Alloys Compd.* **2004**, *375*, 98–106.

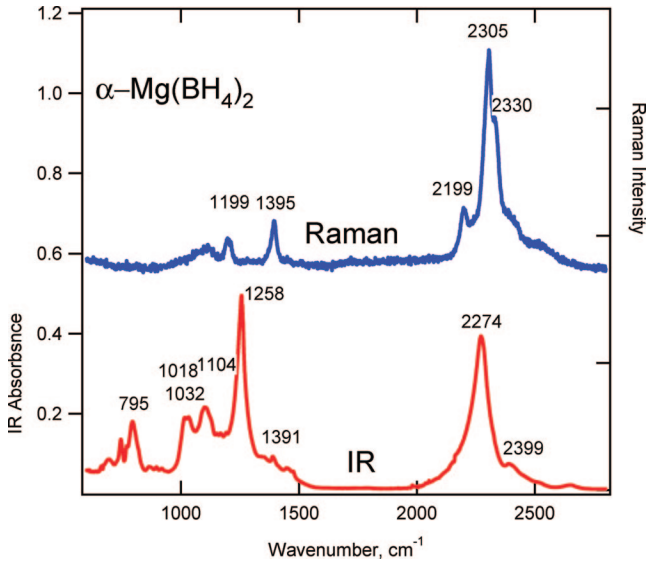

Figure 4. IR and Raman spectra of α-$Mg(BH_4)_2$ at room temperature. The broad feature around 1100 cm^{-1} in the Raman spectrum originates from the glass capillary containing the sample.

cooling and the β-phase becomes quenched at low temperatures. The change of the potential energy landscapes with temperature results in the anomalous behavior of the cell parameters. Therefore, the anomalous cell expansion, indicating unexpected lattice anharmonicity at low temperatures, may be related to the evolution of the free energy profile far from the phase transition temperature. It is interesting to note that the refined atomic displacements in the *Fddd* structure do not detectably decrease as temperature goes down, while for the $P6_122$ structure we observe their pronounced nearly linear decrease.

The closest analogue of $Mg(BH_4)_2$, the recently studied $Ca(BH_4)_2$, also displays a reconstructive transition at high temperatures, and the high-temperature β-phase (space group $P\bar{4}$) can also be easily quenched, but neither this phase nor the low-temperature α- (*F*2*dd*) and α′-phases (*I*-42*d*) show any anomalies of the thermal expansion.[26] Moreover, the β-phase of $Ca(BH_4)_2$ is significantly more dense than the low-temperature phases. None of the structures observed for $Ca(BH_4)_2$, neither the theoretically predicted $I\bar{4}m2$[7] and *F*222[33] structures of $Mg(BH_4)_2$, were observed in our experiments on $Mg(BH_4)_2$.

Vibrational Spectra of Pure $Mg(BH_4)_2$. The vibrational spectra of α-$Mg(BH_4)_2$ at room temperature are shown in Figure 4. The IR spectrum is quite different from the spectra reported by Chłopek et al.,[14] who observed the BH_4 band around 1120 cm^{-1}, while in our spectrum it appears at 1258 cm^{-1}. It is important to note that Chłopek et al. [14] made measurements on KBr pellets, while our experiment is made on the neat sample. A partial substitution of BH_4^- by halide anion has been recently observed in $LiBH_4$.[34] So, it is probable that in the samples described in ref 14 some ion exchange took place, as the υ_4 band in KBH_4 is observed at 1112 cm^{-1}.[32] The Raman shifts corresponding to the internal modes are observed at slightly higher wavenumbers (ca. 5 cm^{-1}) than in our previous study.[3] These new values are more accurate because of a better instrument calibration. The Raman spectrum shown in Figure 4 does not contain $LiBH_4$ impurity bands between 1280 and 1320 cm^{-1}, present in other samples.[3]

The vibrational spectra show the B−H stretching modes around 2300 cm^{-1}, shown to be subject to considerable Fermi resonances,[35] and the BH_4 bending modes between 1000 and 1400 cm^{-1}. Typically, the bands originating from the Raman active ν_2 mode of the isolated tetrahedral molecule are relatively strong in the Raman spectrum and weak in the IR, while the IR and Raman active ν_4 mode is stronger in the IR. The high value of 1395 cm^{-1} component of the ν_2 bending mode can be qualitatively related to the bidentate binding of the BH_4^- molecule to the Mg^{2+} ions; that is, the presence of the Mg ion leads to an increase in frequency of the symmetrical BH_2 bending mode. The origin of the 795 cm^{-1} band seen in the IR spectrum is not clear. We have obtained preliminary temperature dependent Raman spectra of $Mg(BH_4)_2$; however, as soon as the sample undergoes the phase transition at high temperature, a very strong background signal, which does not disappear upon cooling, hinders considerably the collection of usable data.

Conclusions

In this work we have obtained a pure $Mg(BH_4)_2$ sample and characterized it by synchrotron X-ray diffraction and vibrational spectroscopy. The structure of the low-temperature α-phase, originally reported by two independent groups in the space group $P6_1$,[3,4] is revised in the space group $P6_122$, using 100 K single-crystal diffraction data. The revision supports the suggestion made in the DFT study[5] of the $P6_1$ structure. Analysis of the published $P6_1$ models shows that location of the H-atoms from powder data posed the main problem for the identification of the correct symmetry: wrongly determined orientations of some BH_4 groups hampered a successful detection of the true $P6_122$ symmetry by automatic algorithms. On the other hand, the restrained refinement in $P6_122$, using our new high-resolution powder data, allows the accuracy of the single-crystal study to be approached.

Experimentally determined B−H distances are statistically identical, displaying the 1.142 Å mean over 20 independent bond lengths. The experimental average is by 0.082 Å shorter than the theoretical one (1.224 Å [5]). The major part of this difference is due to the displacement of the electron cloud seen by X-rays relative to an average nuclear position,[13] while the contribution of BH_4 libration to the shortening of the B−H bonds is small. To evaluate better the crystal chemistry, the apparent hydrogen atom positions at 100 K were corrected by extending the average experimental B−H bond lengths to the theoretical value. The BH_4 groups are coordinated by Mg atoms via the two opposite edges, but the $Mg-H_2BH_2-Mg$ fragments are not strictly linear: the

(33) Voss, J; Hummelshøj, J. S; Łodziana, Z.; Vegge, T *J. Phys.: Condens. Matter* **2009**, *21*, 012203.
(34) Mosegaard, L.; Moeller, B.; Jorgensen, J.-E.; Filinchuk, Y.; Cerenius, Y.; Hanson, J.; Dimasi, E.; Besenbacher, F.; Jensen, T. *J. Phys. Chem. C* **2008**, *112*, 1299–1303.
(35) Carbonnière, P.; Hagemann, H. *J. Phys. Chem. A* **2006**, *110*, 9927–9933.

Mg−B−Mg angles range from 148 to 170°. H−B−H angles in the Mg−H_2B fragments are in average by 2° more open than for the noncoordinated ones. The DFT model shows the same trend with an even larger difference. A detectable distortion of the tetrahedral BH_4 groups can be attributed to the strong polarizing effect of the Mg^{2+} cation or to a partially covalent Mg−BH_4 interaction.

The dodecahedral MgH_8 coordination of the three independent Mg atoms in α-$Mg(BH_4)_2$ can be described as a slightly distorted snub disphenoid. Four BH_4 groups around each Mg can be grouped in two pairs, each forming a nearly planar BH_2−Mg−H_2B fragment, with the two fragments forming an ∼90° dihedral angle. The shortest H···H distances between the BH_4 groups (2.18−2.28 Å) appear within these BH_2−Mg−H_2B fragments, and they are among the shortest in the structurally characterized metal borohydrides.[30] All other intermolecular H···H contacts in α-Mg-$(BH_4)_2$ are longer than 2.47 Å but typically range from 2.7 to 2.9 Å. The single-crystal study gives a narrow, 1.92−2.16 Å, range of Mg−H distances, which is only slightly broader than the theoretical 2.00−2.13 Å range.

We found that α-$Mg(BH_4)_2$ contains an unoccupied void, overlooked in the previously reported $P6_1$ models, accounting for 6.4% of space in the structure. It is large enough (37 $Å^3$) to accommodate a small molecule, like H_2O. The void forms an infinite channel along the 00z direction, which may provide a path for hydrogen diffusion during initial stages of hydrogen desorption. It is remarkable that by ∼3% less dense high-temperature β-phase contains no unoccupied voids.

A smooth variation of the cell parameters for the α-phase indicates that there is no hypothetical transition from the $P6_122$ structure to $P6_1$ or vice versa, and therefore the structure revision for the hexagonal phase is valid at all temperatures. The α-phase transforms into the β-phase above 490 K; the latter is quenched (metastable) on cooling. The anomalous cell expansion of the β-phase may be related to the evolution of the free energy profile far from the phase transition temperature.

Acknowledgment. This work was partly performed at the Swiss-Norwegian Beam Lines at ESRF, Grenoble, France, and the Swiss Light Source at PSI, Villigen, Switzerland. The authors acknowledge L. Guénée for the help with annealing the sample, D. Chernyshov for valuable discussions, and P. Pattison for critical reading of the manuscript. This work was partly supported by the Swiss National Science Foundation.

Supporting Information Available: Tables of atomic positions determined by different techniques; least-squares planes through atoms; representative Rietveld refinement profiles; and crystal data as CIF files. This information is available free of charge via the Internet at http://pubs.acs.org.

CM803019E